



Osinga, H. M., & Rokni, R. (2003). Numerical study of manifold computations.

Early version, also known as pre-print

[Link to publication record in Explore Bristol Research](#)
PDF-document

University of Bristol - Explore Bristol Research

General rights

This document is made available in accordance with publisher policies. Please cite only the published version using the reference above. Full terms of use are available:
<http://www.bristol.ac.uk/pure/about/ebr-terms.html>

Numerical study of manifold computations

Hinke Osinga

Department of Engineering Mathematics
University of Bristol
Bristol BS8 1TR, UK
H.M.Osinga@bristol.ac.uk

Reza Rokni

School of Mathematical Sciences
University of Exeter
Exeter EX4 4QE, UK
Reza@maths.ex.ac.uk

Abstract

In this paper we study the numerical accuracy of computing one-dimensional manifolds of (non-hyperbolic) equilibria in a planar vector field for which the manifolds are known explicitly. We consider the (strong) stable manifolds of a saddle, a sink, and a centre-stable equilibrium.

Introduction

The numerical approximation of stable or unstable manifolds is often used as a tool to investigate the global behaviour of a dynamical system. Most methods are designed for manifolds of hyperbolic equilibria and utilize the fact that integration can be done such that the manifold is (locally) an attractor. This means that a bounded approximation of the manifold can be computed as close to the true manifold as one likes. In this paper, we consider the cases where a one-dimensional (strong) stable manifold of a vector field is computed. This necessarily implies that it is the manifold of an equilibrium. We consider both hyperbolic and non-hyperbolic equilibria.

The standard method to compute the one-dimensional stable manifold of an equilibrium in a vector field is to choose a point on the local manifold close to the equilibrium and integrate it backward in time; for example, see [3]. Most methods use the linear manifold as an approximation for the local manifold, because the (strong) stable manifold is tangent at the equilibrium to the corresponding (strong) stable eigenspace [2]. Our investigations use this method as well.

If the equilibrium is hyperbolic and has only a one-dimensional stable manifold, then this manifold is an attractor in backward time, at least locally near the equilibrium. This means that initially the distance of points on the computed trajectory to the true manifold decays. This property is utilized to show that the computational error decays to zero as $\delta \rightarrow 0$, even though the integration time that is needed to reach a specific finite arclength evidently goes to infinity in the process; see [4].

If one considers a vector field with an equilibrium that is not hyperbolic, or if one is interested in finding the strong stable manifold of an equilibrium with more than one stable eigenvalue, then standard error bounds no longer apply. In this paper we investigate how the maximum error varies with δ using a two-dimensional vector field for which the manifolds are known explicitly. We consider the hyperbolic saddle, the hyperbolic sink and the case where the equilibrium has one zero and one stable eigenvalue.

Explicit manifolds

We consider an example for which the (strong) stable manifold is known explicitly, namely

$$\begin{cases} \dot{x} &= \alpha x, \\ \dot{y} &= \beta y + \gamma x^2, \end{cases} \quad (1)$$

with the explicit solution

$$\begin{cases} x(t) &= x_0 e^{\alpha t}, \\ y(t) &= \frac{\gamma}{2\alpha - \beta} x_0^2 e^{2\alpha t} + \left(y_0 - \frac{\gamma}{2\alpha - \beta} x_0^2 \right) e^{\beta t}. \end{cases} \quad (2)$$

Here we assume that $\alpha < 0$ and $\beta > \alpha$, so that the origin has at least a one-dimensional stable manifold. Note that this automatically ensures that $2\alpha - \beta \neq 0$. If $\beta > 0$, then the origin is a saddle and we can immediately see from (2) that trajectories with initial condition $(x_0, y_0) \in \mathbb{R}^2$ go to the origin if and only if

$$y_0 = \frac{\gamma}{2\alpha - \beta} x_0^2. \quad (3)$$

Hence, Eq. (3) defines the stable manifold $W^s(0)$ of the origin. Similarly, if $\beta = 0$, the origin is non-hyperbolic with a strong stable manifold defined by Eq. (3). In fact, here any point on the y -axis is an equilibrium and they all have one stable and one zero eigenvalue. A system of this type is of interest, for example, in adaptive control theory [5].

Let us now assume that $\alpha < \beta < 0$, so that the origin is stable with a one-dimensional strong stable manifold. Since both α and β are negative, all solutions go to the origin. However, since the attraction in the x -direction is stronger than in the y -direction, most solutions converge to the origin tangent to the y -axis. The only exception are the solutions on the strong stable manifold $W^{ss}(0)$, which is tangent to the x -axis at the origin. Hence, we are looking for solutions with $\frac{dy}{dx}(t) \rightarrow 0$ as $t \rightarrow \infty$. For $x_0 \neq 0$, we have

$$\begin{aligned} \frac{dy}{dx}(t) = \frac{\dot{y}(t)}{\dot{x}(t)} &= \frac{\beta y(t) + \gamma x(t)^2}{\alpha x(t)} \\ &= \frac{\frac{\beta\gamma}{2\alpha - \beta} x_0^2 e^{2\alpha t} + \beta \left(y_0 - \frac{\gamma}{2\alpha - \beta} x_0^2 \right) e^{\beta t} + \gamma x_0^2 e^{2\alpha t}}{\alpha x_0 e^{\alpha t}} \\ &= \frac{2\gamma}{2\alpha - \beta} x_0 e^{\alpha t} + \frac{\beta}{\alpha x_0} \left(y_0 - \frac{\gamma}{2\alpha - \beta} x_0^2 \right) e^{(\beta - \alpha)t}. \end{aligned}$$

Since $\alpha < \beta < 0$ and thus $e^{(\beta - \alpha)t} \rightarrow \infty$ as $t \rightarrow \infty$, the strong stable manifold is again defined by Eq. (3).

Throughout this paper, we choose $\gamma = \beta - 2\alpha$ such that the (strong) stable manifold is always given by the graph of the function $y = -x^2$.

Numerical approximations

Our aim is to compute the (strong) stable manifold of the origin for our example (1) with appropriate choices of $\alpha < 0$, $\beta > \alpha$ and $\gamma = \beta - 2\alpha$. The linear (strong) stable manifold is the x -axis. Hence, we approximate the branch $\{(x, \frac{\gamma}{2\alpha - \beta} x^2) \mid x > 0\}$ up to arclength L by the horizontal segment from the origin to $(\delta, 0)$ followed by the backward-time trajectory through $(\delta, 0)$, where $\delta > 0$ is small. We use fourth-order Runge-Kutta integration with fixed step size $h = 10^{-5}$ to approximate such a trajectory. This obviously introduces an integration error, but it appears to be negligible in our computations. Note that the total integration time needed to reach arclength L increases as δ decreases.

The numerical approximation consists of a finite set $M_\delta(L) = \{(x_i, y_i)\}_{i=0}^N$ of integration points, where (x_0, y_0) is the origin, $(x_1, y_1) = (\delta, 0)$ and N is the total number of integration steps such that (x_N, y_N) is the first point along the trajectory for which the approximate arclength distance to the origin is at least L . To keep the total number of points in $M_\delta(L)$ small, we consider only a subset of the integration mesh points such that we maintain a good resolution of the curve. We ensure that the angle formed by any three consecutive points does not exceed a prescribed maximum $\alpha_{max} = 0.3$. Furthermore, the product of this angle with the distance between the last two of these three points never exceeds $(\Delta\alpha)_{max} = 10^{-9}$. In practice, this means that points will be distributed according to curvature, while the bound $(\Delta\alpha)_{max}$ ensures a small interpolation error. For ease of notation, this reduced set of mesh points is still denoted by $M_\delta(L)$, and it contains N_L points, where typically, $N_L \ll N$.

The piecewise linear curve through the mesh points in $M_\delta(L)$ forms the approximate (strong) stable manifold. The distance of this approximation to the true manifold is considered pointwise. For convenience, we only consider the difference in the y -coordinate. Hence, we define the error of our computation as

$$\text{dist}(M_\delta(L), W^s(0)) = \max_{0 \leq i < N_L} \left| y_i - \frac{\gamma}{2\alpha - \beta} x_i^2 \right|.$$

Given how we compute the approximate manifold, this error depends on the initial point $(\delta, 0)$ and on the arclength L of the computation.

We consider three different cases, namely the case of a hyperbolic saddle, a hyperbolic sink and a non-hyperbolic centre-stable equilibrium. For each case we compute approximations of the (strong) stable manifold up to arclength $L = 3$ with $\delta = 0.001$. Figure 1 shows the behaviour of the pointwise error as a function of the arclength distance to the origin for all three cases. The stable manifold of the hyperbolic saddle is an attractor in backward time. Hence, the first point $(\delta, 0)$ of the backward trajectory is furthest away from the true manifold (namely $10^{-6} = |-\delta^2|$), because the trajectory converges to the manifold. In contrast, the strong stable manifold of a hyperbolic sink is a repeller in backward time. The largest error now occurs at the last integration point. The error along the stable manifold of the centre-stable equilibrium does not change at all.

Let us now study how the maximum error depends on δ . For each case we calculate manifolds $M_\delta(L)$ with $L = 3$ fixed throughout, while δ varies. For $L = 3$, the reduced mesh of $M_\delta(L)$ consists of $N_L \approx 130\,000$ points, even though the required integration time may grow as large as one million.

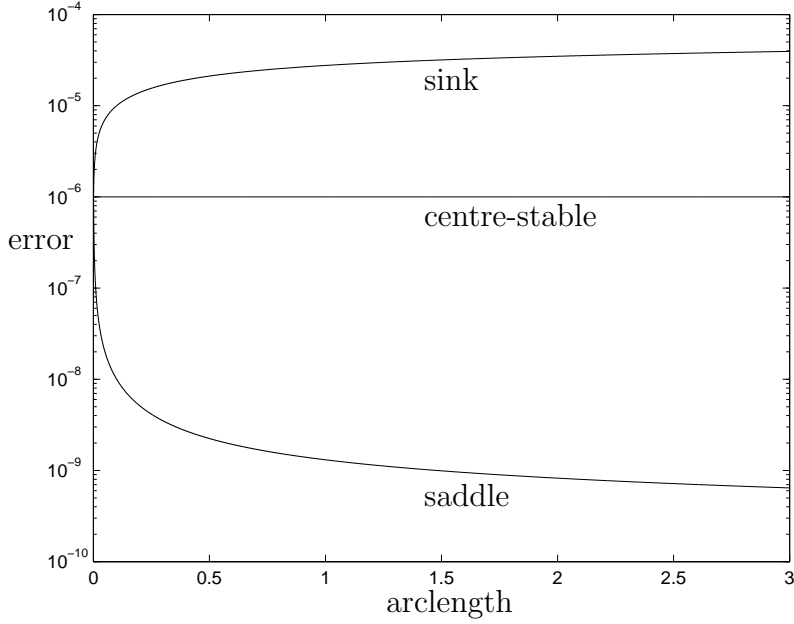


Figure 1: *The pointwise error versus arclength distance to the origin of approximate (strong) stable manifolds $M_\delta(L)$ for the hyperbolic saddle, the hyperbolic sink and the centre-stable equilibrium; for all cases $\delta = 0.001$ and $L = 3$.*

δ	10^{-1}	10^{-2}	10^{-3}	10^{-4}	10^{-5}
error saddle	10^{-2}	10^{-4}	10^{-6}	10^{-8}	10^{-10}
error centre	10^{-2}	10^{-4}	10^{-6}	10^{-8}	10^{-10}
error sink	$3.95 \cdot 10^{-2}$	$1.25 \cdot 10^{-3}$	$3.94 \cdot 10^{-5}$	$1.25 \cdot 10^{-6}$	$3.94 \cdot 10^{-8}$

Table 1: *Approximations of the (strong) stable manifold of the origin in (1) up to arclength $L = 3$. For the hyperbolic saddle $(\alpha, \beta, \gamma) = (-1, 1, 3)$, for the non-hyperbolic centre-stable equilibrium $(\alpha, \beta, \gamma) = (-1, 0, 2)$, and for the hyperbolic sink $(\alpha, \beta, \gamma) = (-2, -1, 3)$.*

Hyperbolic saddle

The origin in example (1) is a hyperbolic saddle for $\alpha = -1$, $\beta = 1$ and $\gamma = 3$. Note that the parameters are such that $W^s(0)$ is defined as the graph of Eq. (3).

The second row in Table 1 shows the results of our computations when varying δ from 10^{-1} to 10^{-5} . The error decreases quadratically with δ ; see also Fig. 2. This behaviour is as expected, because the largest error is always at the initial point.

Centre-stable equilibrium

The origin in example (1) has one zero and one stable eigenvalue for $\alpha = -1$, $\beta = 0$ and $\gamma = 2$. Note that this example is degenerate: the y -axis is invariant and consists entirely of non-hyperbolic equilibria. Hence, it is not surprising that the computational

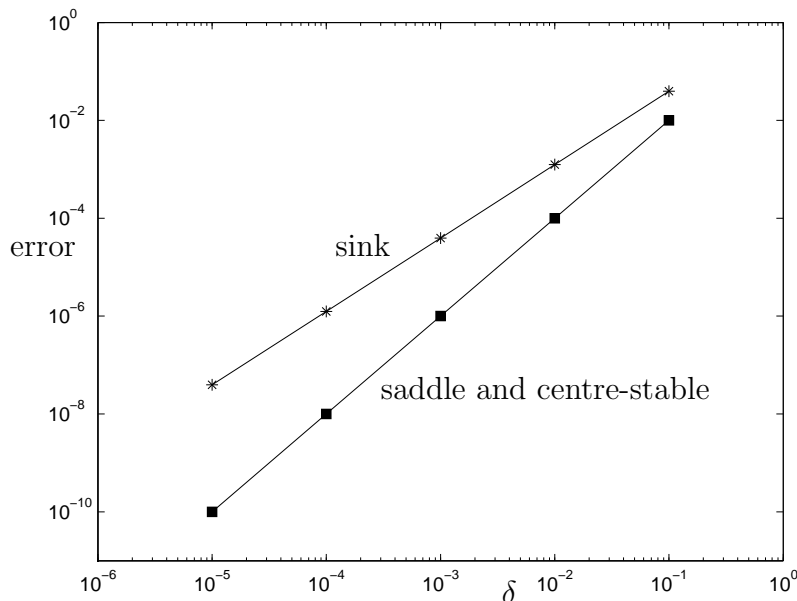


Figure 2: *The maximal error $\text{dist}(M_\delta(L), W^s(0))$ as a function of δ with $L = 3$ for the hyperbolic saddle, the hyperbolic sink and the centre-stable equilibrium (same as the saddle).*

error remains the same along the entire manifold. (This also shows that the integration error is small enough so that it is negligible.)

The maximal error behaves exactly the same as for the case of the hyperbolic saddle; see Table 1. Hence, again, the error decreases quadratically with δ .

Hyperbolic sink

Example (1) has a hyperbolic sink at the origin for $\alpha = -2$, $\beta = -1$ and $\gamma = 3$.

Since the strong stable manifold is a repeller in backward time, we now find that the largest error is at the last computed point. The maximal error depends on δ as shown in the last row of Table 1. We see that, as before, the error decreases with δ . More precisely, when δ decreases by a factor 10, the error decreases by a factor $3.16 \cdot 10^{-2}$. The quantitative differences with the hyperbolic saddle are best seen in a log log-plot of the error versus δ as visualised in Fig. 2.

For this example it is also of interest to investigate how the error depends on the arclength L , because the largest error is always at the last integration point. We computed approximations of the strong stable manifold using the same variations for δ , but now also varying L from 10^0 to 10^4 . The maximal error, i.e. the distance in the y -direction of the last computed point to the true manifold, is shown in Table 2.

As before, for fixed arclength the error decreases by a factor $3.16 \cdot 10^{-2}$ when δ is decreased by a factor 10. That is, the contraction rate across the rows in Table 2 is constant. The contraction rate across the columns in Table 2 is also fairly constant. Namely, when the arclength is reduced by a factor 10, the error decreases by a factor 0.56. This reduction rate is slightly smaller (no less than 0.5) when L is relatively small.

	$\delta = 10^{-1}$	$\delta = 10^{-2}$	$\delta = 10^{-3}$	$\delta = 10^{-4}$	$\delta = 10^{-5}$
$L = 10^0$	$2.77 \cdot 10^{-2}$	$8.74 \cdot 10^{-4}$	$2.76 \cdot 10^{-5}$	$8.74 \cdot 10^{-7}$	$2.76 \cdot 10^{-8}$
$L = 10^1$	$5.52 \cdot 10^{-2}$	$1.74 \cdot 10^{-3}$	$5.51 \cdot 10^{-5}$	$1.74 \cdot 10^{-6}$	$5.51 \cdot 10^{-8}$
$L = 10^2$	$9.98 \cdot 10^{-2}$	$3.15 \cdot 10^{-3}$	$9.97 \cdot 10^{-5}$	$3.15 \cdot 10^{-6}$	$9.97 \cdot 10^{-8}$
$L = 10^3$	$17.78 \cdot 10^{-2}$	$5.62 \cdot 10^{-3}$	$17.78 \cdot 10^{-5}$	$5.62 \cdot 10^{-6}$	$17.78 \cdot 10^{-8}$
$L = 10^4$	$31.62 \cdot 10^{-2}$	$10.00 \cdot 10^{-3}$	$31.62 \cdot 10^{-5}$	$10.00 \cdot 10^{-6}$	$31.64 \cdot 10^{-8}$

Table 2: *Example (1) with $(\alpha, \beta, \gamma) = (-2, -1, 3)$: Errors of approximations of the strong stable manifold of the origin for varying arclengths L and initial points $(\delta, 0)$.*

Discussion

The example that we consider in this paper is constructed so that the manifolds are known explicitly. This necessarily means that the vector field is relatively simple and the computational error of finding the (strong) stable manifolds behaves extremely regular.

In general, one should compute two or more approximations while varying δ and consider the contraction rates of these successive approximations. Such relative errors and contraction rates give a good idea of the behaviour of the true error and even give information about the size of this error. It is our experience that the contraction rate of the error for more general C^2 vector fields is still of order 10^{-2} ; see [1].

Standard error bounds on integration routines predict that the error increases exponentially with integration time. Indeed, when taking into account integration time in the distance calculations, this may well be true, but we are interested in the *geometric* distance between the manifolds. Hence, in practice, the standard error bounds are nowhere near the actual error. For extremely small δ , i.e. very large integration time, one expects that the integration error will start to have an effect and the approximation error will probably not converge to 0. However, our computations show that approximations with errors of the order 10^{-8} are certainly reasonable to expect.

References

- [1] H.M. Osinga, G.R. Rokni-Lamooki, S. Townley, “Numerical approximations of strong (un)stable manifolds,” Applied Nonlinear Mathematics Preprint 2002.19, University of Bristol, 2002.
- [2] J. Palis and W. de Melo, *Geometric Theory of Dynamical Systems*, Springer-Verlag, 1982.
- [3] T.S. Parker and L.O. Chua, *Practical Numerical Algorithms for Chaotic Systems*, Springer-Verlag, 1989.
- [4] A.M. Stuart and A.R. Humphries, *Dynamical Systems and Numerical Analysis*, Cambridge University Press, 1996.
- [5] S. Townley, “An example of a globally stabilizing adaptive controller with a generically destabilizing parameter estimate,” *IEEE Trans. Automat. Control* **44**(11): 2238–2241, 1999.